arXiv:1512.07746v1 [cond-mat.str-el] 24 Dec 2015

Magnetic Reconstructions in B-site Doped Manganites

Kalpataru Pradhan
CMP Division, Saha Institute of Nuclear Physics, 1/AF Bidhan Nagar, Kolkata 700064, India

The magnetic nature of the B-site dopants controls the magnetic phases in B-site doped manganites $RE_{1-x}AE_xMn_{1-\eta}B_\eta O_3$. Different B-site dopants of equal valence, doped into the same reference manganite, lead to different magnetic phases at low temperature, which can not be explained using the valence change scenario. We focus on trivalent B-site dopants in CE-CO-OO-I manganites at half-filling $x = 0.50$ to study the role of magnetic interactions between the B-site dopants and the neighboring Mn-sites by using a two-orbital double-exchange model including super-exchange interactions, Jahn-Teller lattice distortions and substitutional disorder in two dimensions. We show that the magnetic reconstructions around the B-site dopants due to the modified double-exchange and super-exchange interactions control the phase competition in B-site doped manganites.

In manganites[1–3], $RE_{1-x}AE_xMnO_3$ (RE and AE denote rare-earth and alkaline-earth elements), A-site disorder[4,5] is unavoidable except in few cases of specific doping x and special growth technique[6,7]. A colossal response in a magnetic field emerges due to the A-site disorder which promotes phase coexistence and metal-insulator transition[8,9]. Similar phase coexistence scenario have also been observed in B-site doped manganites $RE_{1-x}AE_xMn_{1-\eta}B_\eta O_3$ where a few percentage of Mn-sites are replaced by foreign elements named B-site dopants [10–20]. In addition, the B-site disorder can tune a ferromagnetic (FM) metal to an anti-ferromagnetic (AF) insulator[16,18] or vice-versa[11]. This promotion of a competing ordered phase has no equivalent in the case of A-site disorder.

In few cases the B-site dopant driven transition from a FM-M to a charge ordered insulator or the reverse transition can be explained using the valence change scenario[21]. Here the Mn valence changes to $3 + \nu$ for an α-valent B-dopant in the reference manganites $RE^{3+}_{1-x}AE^{2+}_xMn^{3+\nu}_{1-\eta}B^{\alpha}_\eta O^{2-}_3$, where the charge neutrality requirement, $\nu(\eta, \alpha, x) = (x + \eta(3 - \alpha))/(1 - \eta)$. The new effective hole density $x_{eff} = \nu$. Significantly, all B-site doped experiments *can not* be explained by the valence change argument as some B-site dopants, particularly the magnetic ones with same valency behave differently[11,12,22]. This requires a careful analysis of magnetic interactions between the B-site dopants and the neighboring Mn-sites.

Our focus is mainly on 3+ dopants in a CE-CO-OO-I (CO:charge order; OO:Orbital order; I: Insulator) manganite at $x = 0.50$. Some elements from our 3+ dopants may exist in 2+ state due to the presence of mixed valence, but that will not affect the qualitative results of this paper. Let us briefly discuss the available experimental data that emphasize the magnetic character of the B-site dopants. The FM-M ground state in Cr doped $La_{0.5}Ca_{0.5}MnO_3$ (LCMO)[12] cannot be explained using the valence change argument. With Cr, a 3+ dopant, the hole density of the manganite *increases* from the initial $x = 0.50$ but there is no FM-M phase which has hole density greater than $x = 0.50$ [2] in LCMO. When $Nd_{0.5}Ca_{0.5}MnO_3$ (NCMO), another CE-CO-OO-I with smaller bandwidth than LCMO, doped with Cr, shows coexistence of FM-M and CO-I phases at low temperature[11,15]. There is no FM phase for $x > 0.5$ in NCMO either. Both these parent manganites have FM-M phases at $x < 0.50$. Dark field images at temperatures below the transition temperature shows that the hole density in the FM domains is less than $x = 0.50$ [12]. This is surprising because the valence change on doping 3+ dopants is in a direction opposite to the clean ferromagnetic (FM) phase, so Cr doping should not have led to a FM-M. In addition to Cr, Ni and Co also lead to ferromagnetism at low temperature when doped into NCMO, going against the valence change scenario. Note, however, that 3+ dopants like Fe, Al, and Sc when doped into the same manganite at $x = 0.50$ do not induce ferromagnetism at any temperature as shown in the left hand side of the Fig-1 [from ref. 15]. Cr, Ni, and Co also induces ferromagnetism at low temperature at the expense of AF ground state in $Pr_{0.5}Ca_{0.5}MnO_3$ (PCMO)[22].

In this letter, we analyze the importance of magnetic interactions between the B-site dopants and the neighboring Mn-sites to understand different magnetic phases at the low temperature. The magnetic reconstructions around the B-site dopants control the phase competition between the FM and the AF phase. We explain the origin of two type of magnetic reconstructions that induces ferromagnetism in an AF insulator. We use a two-dimensional model Hamiltonian for manganites with B-site dopants in the limit $J_H \to \infty$ [23]. The model is given by

$$\begin{aligned}
H_{tot} &= H_{ref} + H_{imp}, \text{ where} \\
H_{ref} &= \sum_{\langle ij\rangle\sigma}^{\alpha\beta} \tilde{t}^{ij}_{\alpha\beta} d^\dagger_{i\alpha\sigma} d_{j\beta\sigma} + J \sum_{\langle ij\rangle} \mathbf{S}_i.\mathbf{S}_j \\
&\quad - \lambda \sum_i \mathbf{Q}_i.\boldsymbol{\tau}_i + \frac{K}{2} \sum_i \mathbf{Q}_i^2 \text{ and} \\
H_{imp} &= V \sum_{n\alpha\sigma} d^\dagger_{n\alpha\sigma} d_{n\alpha\sigma} + J' \sum_{\langle nj\rangle} \mathbf{S}_n.\mathbf{S}_j + V_c \sum_{\langle nj\rangle} q_n q_j.
\end{aligned}$$

The reference 'manganite model' H_{ref} involves the nearest neighbor hopping of e_g electrons with ampli-

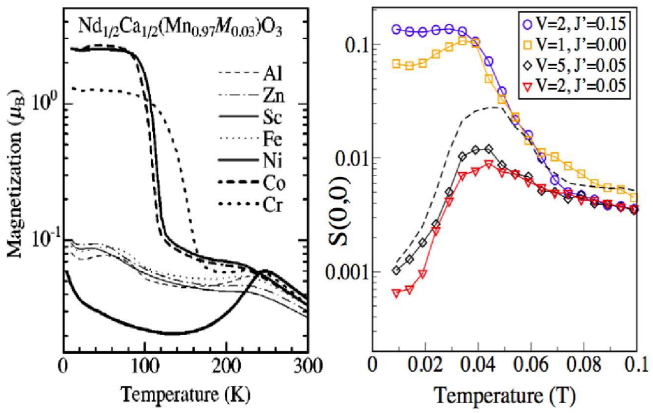

FIG. 1: Left: Temperature dependence of magnetization for different B-site dopants in $Nd_{0.5}Ca_{0.5}MnO_3$. Magnetization is measured under a field of 0.5 T [results from A. Machida, *et al.*, Phy. Rev. B **65**, 064435 (2002)]. Right: Temperature dependence of the FM peak $[S(\mathbf{0},\mathbf{0})]$ for four representative parameter points in the phase diagram (Fig-2) with $h = 0.002$ (lattice size: 24×24). The dotted line is for the reference CE-CO-OO-I phase.

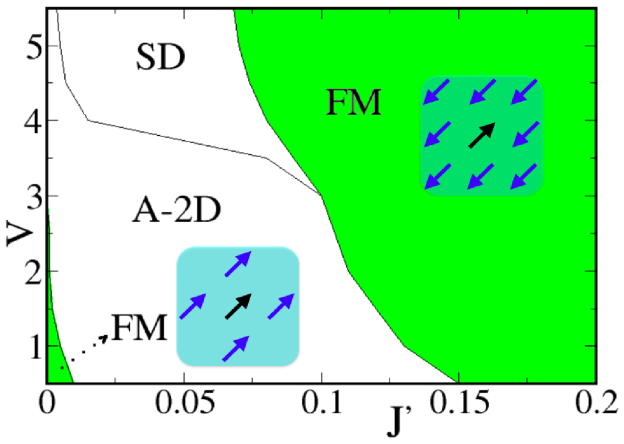

FIG. 2: Low temperature (T = 0.01) 'phases' at $x = 0.50$ for varying V and J' for 3+ B-site dopants in a external magnetic field $h = 0.002$. We have taken $\lambda = 1.6$ and $J = 0.1$. There are two regions in the phase diagram where ferromagnetism is induced. The other regions are either spin disordered phase or mostly A-2D type phase.

tude $\tilde{t}^{ij}_{\alpha\beta}$ (two orbitals a and b), anti-ferromagnetic (AF) super-exchange (SE) J between Mn t_{2g} spins, and Jahn-Teller (JT) interaction λ between the electrons and the phonon modes $\mathbf{Q}_i$ in the adiabatic limit. The hopping amplitudes $\tilde{t}^{ij}_{\alpha\beta}$ depend upon the orientations of t_{2g} spins at sites i and j where $\tilde{t}^{ij}_{\alpha\beta} = \Theta_{ij} t^{ij}_{\alpha\beta}$ with $\Theta_{ij} = \cos(\theta_i/2)\cos(\theta_j/2) + \sin(\theta_i/2)\sin(\theta_j/2)e^{-i(\phi_i-\phi_j)}$. We treat all t_{2g} spins and phonon degrees of freedom as classical[24], and measure all energies in units t_{aa}=1. We set stiffness of the JT modes, K=1 and $|\mathbf{S}_i| = 1$. The overall carrier density is controlled through the chemical potential. For details please see Ref. 21,23,25

We use an exact diagonalization method to the e_g electrons in the presence of the t_{2g} spins and the phonon modes (Q). A Monte Carlo (MC) technique based on the 'travelling cluster approximation' (TCA)[26] is employed to access large system sizes[25,27–29]. H_{ref} reproduce the correct sequence of magnetic phases in the 'clean' manganites for $J = 0.1$ and $\lambda = 1.6$ [21].

The CE-CO-OO-I phase is stable only at $x = 0.50$ for $\lambda = 1.6$ and $J = 0.1$ [25,30]. There are phase separation windows (as shown in Fig-2 of Ref. 21) on both sides of the $x = 0.50$ CE-CO-OO-I phase e.g., anti-ferromagnetic A-type phase (A-2D) phase for $x \geq 0.55$ and FM-M phase for $x \leq 0.40$. A few percentage of 3+ dopants at $x = 0.50$ will shift the x_{eff} into the phase separation region between $x = 0.50$ and $x = 0.55$ creating a mixture of A-2D and CE-type phase without any ferromagnetic correlations. The valence change argument may be the correct way to explain the very weak ferromagnetic feature when Fe, Al or Ga dopants are introduced into NCMO (see left side of Fig-1). But, the mystery is why some trivalent/divalent dopants like Cr and Ni induce ferromagnetism in the CE-CO-OO-I phase, while other 3+ dopants such as Fe unable to do so.

We modifiy the local physics around the B-site dopant. In principle the SE interaction between the B-Mn sites can be very different from the SE interaction between the Mn-Mn sites. The position of the impurity level at the B-site dopant also makes a difference since it controls double-exchange (DE) driven ferromagnetic coupling between the B-Mn sites. Another important aspect is short-range Coulomb interaction between the B-site dopant and the neighboring Mn site, particularly when charge ordered reference states are considered. When a B-site dopant is introduced into a CE-CO-OO-I state the fixed charge state of the B-site dopant forces a rearrangement in the valence of the neighboring Mn to minimize the Coulomb repulsion[31]. For instance, a 3+ dopant like Cr is more likely to be surrounded by Mn^{4+} ions. H_{imp} contains these three changes in the model due to the B-site dopants; i) the B-site dopant e_g states placed at an energy V above the center of the Mn band, ii) the SE coupling is modified to J' between the B-site moments S_n and the neighboring Mn moments, and iii) a nearest neighbor (NN) Coulomb repulsion V_c between the B-site dopant and the neighboring Mn sites is added [21]. We assume $V_c = 0.1$ in our calculation[31,32]. The quantitative physics does not change without the NN Coulomb repulsion ($V_c = 0$).

The two parameters V and J' define our minimal set to tune the effective magnetic interaction between the B-site dopants and neighboring Mn-sites. Fig-2 shows the phase diagram of the B-site doped CE-CO-OO-I for different combinations of V and J'. We set $\eta = 0.08$, and have used a small external magnetic field $h = 0.002$ as in the experiments (see Fig-1). In an external magnetic field a Zeeman coupling $H_{mag} = -h \cdot \sum_i \mathbf{S}_i$ is added to

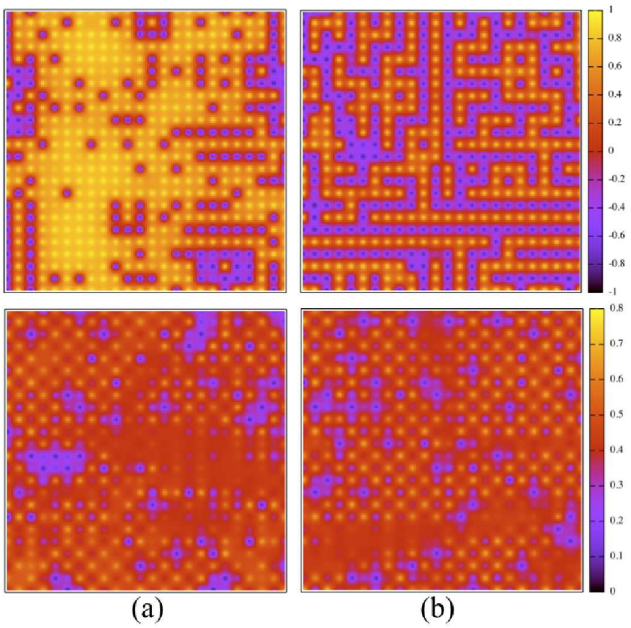

FIG. 3: The z components of the t_{2g} spins (top row) and the electron density (bottom row) for each site on a 24×24 lattice at T = 0.01 ($\eta = 0.08$). (a) $V = 2$ and $J' = 0.15$, (b) $V = 5$ and $J' = 0.05$.

the Hamiltonian. We find two unexpected FM regions, one at lower J' and V values, the other at higher values of J'. The non-ferromagnetic region is divided into two parts: i) A-2D type correlations and ii) spin disordered (SD) like phase.

We believe that the ferromagnetism at large SE regime is due to the complex structure of CE-CO-OO-I phase. The Mn^{3+} (or Mn^{4+}) ion in CE-CO-OO-I phase (checkerboard arranged Mn^{3+} and Mn^{4+} ions) has two NN spins aligned parallel to it and other two NN spins aligned anti-parallel to it. For Mn^{3+}, out of four next NN spins, two are parallel and other two are anti-parallel to the central Mn spin. Due to large J' at B-site, all the neighboring Mn spins align anti-parallel to the B-site moment. To gain kinetic energy along a '1+8' ring all four next NN align anti-parallel to the B-site as shown in the inset of Fig-2. For Mn^{4+}, all four next NN are already aligned anti-parallel to it. At large enough impurity concentration the FM '1+8' rings align in the same direction to promote FM correlations in a AF phase. Notice, this argument does not involve the valence of the dopant.

Along with the AF coupling J', the other crucial effect comes from the short range Coulomb repulsion V_c. Due to this 3+ B-site dopants prefer Mn^{4+} ions as nearest neighbors. The effective hole density increases with 3+ dopant but most of the low electron density (high hole density) sites are close to the B-site dopants. Some sites with high electron density (low hole density) club together in impurity free patches. The overall pattern that emerges is a complex mixture of FM-M and AF regions. Fig-3 (a) shows the z components of t_{2g} spins and the electron density for each site from MC snapshots for $\eta = 0.08$. The MC snapshot shows ferromagnetic patches and we found that the effective hole density of these ferromagnetic patches are less than 0.50, but are weakly charge ordered, unlike in the experiment [12]. This ferromagnetism is purely due to the magnetic and the electronic reconstructions around the B-site dopants. We believe that the magnetic reconstructions also lead to ferromagnetism in Cr doped off-half-filled manganites *e.g*, $(La_{0.3}Pr_{0.7})_{0.65}Ca_{0.35}Mn_{1-\eta}Cr_\eta O_3$ [19], $La_{0.4}Ca_{0.6}Mn_{1-\eta}Cr_\eta O_3$ [20].

For lower V and J' values there is another narrow ferromagnetic window. For lower J', B-site dopant connects to nearest neighbors Mn-sites ferromagnetically in the absence of significant SE interaction. This FM alignment is due to the gain in DE energy for smaller V values. In the present case, clusters of '5 sites' spins forms a large magnetic moment, as shown in the inset of Fig-2. This '5 sites' spin structure is the building block for ferromagnetism in this regime. In fact, a ferromagnetic SE interaction will broaden this ferromagnetic region. As the impurity level (V) grows the FM phase gets quickly suppressed due to the reduction in the DE energy gain.

In the phase diagram there is no ferromagnetic phase at higher V and lower J' values. In this case the system cannot generate either a cluster of '5 sites', or the '1 + 8' ferromagnetic configuration. The spin disordered (SD) region is a complex mixture of A-2D phase and the CE phase. Fig-3 (b) shows the z components of t_{2g} spins and electron density for each site for $V = 5$ and $J' = 0.05$. There is no significant ferromagnetic correlations. Other dominant phase (for lower V and intermediate J' values) is A-2D type phase. This phase is expected due to the valence change scenario discussed earlier.

It clear from the experiments[15,22] that doping Al, Fe, Ga, and Sc (say type-I) in CE-CO-OO-I manganite do not induce any ferromagnetism, whereas Cr, Ni, and Co (say type-II) lead to ferromagnetism at low temperature at the expense of AF ground state. Type-I dopants either have d^0 or d^{10} configuration except Fe which has d^5 electronic configuration while d orbitals are partially occupied in type-II dopants. Based on the electronic configuration 3+ dopants can be divided into magnetic and non-magnetic. Magnetic dopants interact magnetically with their neighboring Mn-sites. Experimental result suggests that Cr interacts antiferromagnetically to the Mn-sites whereas Ni couples ferromagnetically[33]. Fe is magnetic but interacts weakly with the Mn-sites due to its stable d^5 configuration[34] and this may be the cause for the absence of ferromagnetism on Fe doping. Other dopants like Al, Sc, and Ga which do not have partially filled d electrons are categorized as non-magnetic. These non-magnetic dopants do not have any magnetic interaction (valid for large V and $J' = 0$) with Mn-sites. The physics due to the valence change scenario dominates for these non-magnetic 3+ dopants and there is no ferromagnetism, as observed in experiments[14,15]. Taking all these observation into consideration we classify different

	$V and J'$	**Dopants (similar to)**	d **electrons**	**Type**
(i)	$V = 2, J' = 0.15$	Cr like	d^3	Magnetic
(ii)	$V = 1, J' = 0.00$	Ni like	d^7	Magnetic
(iii)	$V = 5, J' = 0.05$	Fe like	d^5	Magnetic
(iv)	$V = 5, J' = 0.00$	Ga/Al like	d^0	Non-Magnetic

TABLE I: Various parameter V and J' to mimic different B-site dopants in experiments.

dopants in Table-1.

To draw parallel with the experiments we show ferromagnetic structure factor $S(\mathbf{0,0})$ (thermal average combined with an additional average overten different 'samples') with temperature for four combinations of V and J' values to probe different parts of the phase diagram in Fig-1. Only first two combinations [$V = 2, J' = 0.15$ (Cr like); $V = 1, J' = 0.00$ (Ni like)] show significant ferromagnetism at low temperature while the other two have negligible ferromagnetic correlations.

In conclusion, we explained the non-trivial effect of B-site dopants on a CE-CO-OO-I phase. Although valence change is in opposite direction with respect to the FM-M phase, the magnetic reconstructions create large magnetic patches and induce ferromagnetism for Cr/Ni like dopants. We also show that there are two types of magnetic reconstructions that induce ferromagnetism depending upon the magnetic interaction between the B-site dopants and the Mn-sites. We crudely guessed the value of SE interaction between the B-site dopants and neighboring Mn-sites, but we believe one can extract this value from first principle calculations.

We acknowledge our discussions with Pinaki Majumdar and Anamitra Mukherjee.

[1] E. Dagotto, Science, **309**, 257 (2005).
[2] *Colossal Magnetoresistive Oxides*, edited by Y. Tokura (Gordon and Breach, New York, 2000).
[3] Y. Tokura, Rep. Prog. Phys. **69**, 797 (2006).
[4] L. M. Rodriguez-Martinez and J. P. Attfield, Phys. Rev. **B 58**, 2426 (1998).
[5] L. M. Rodriguez-Martinez and J. P. Attfield, Phys. Rev. **B 63**, 024424 (2001).
[6] D. Akahoshi, M. Uchida, Y. Tomioka, T. Arima, Y. Matsui, and Y. Tokura, Phys. Rev. Lett. **90**, 177203 (2003).
[7] R. Mathieu, D. Akahoshi, A. Asamitsu, Y. Tomioka, and Y. Tokura, Phys. Rev. Lett. **93**, 227202 (2004).
[8] A. Moreo, M. Mayr, A. Feiguin, S. Yunoki, and E. Dagotto, Phys. Rev. Lett. **84**, 5568 (2000).
[9] S. Kumar and P. Majumdar, Phys. Rev. Lett. **92**, 126602 (2004).
[10] T. Kimura, Y. Tomioka, R. Kumai, Y. Okimoto, and Y. Tokura, Phys. Rev. Lett. **83**, 3940 (1999).
[11] T. Kimura, R. Kumai, Y. Okimoto, and Y. Tomioka, Phys. Rev. B **62**, 15021 (2000).
[12] Y. Moritomo, A. Machida, S. Mori, N. Yamamoto, and A. Nakamura, Phys. Rev. B **60**, 9220 (1999).
[13] S. Mori, R. Shoji, N. Yamamoto, T. Asaka, Y. Matsui, A. Machida, Y. Moritomo, and T. Katsufuji, Phys. Rev. **B 67**, 012403 (2003).
[14] Y. Moritomo, K. Murakami, H. Ishikawa, M. Hanawa, A. Nakamura, and K. Ohoyama, Phys. Rev. B **69**, 212407 (2004).
[15] A. Machida, Y. Moritomo, K. Ohoyama, T. Katsufuji, and A. Nakamura, Phy. Rev. **B 65**, 064435 (2002).
[16] K. H. Ahn, X. W. Wu, K. Liu, and C. L. Chien, J. Appl. Phys. **81**, 5505 (1997).
[17] A. Barnabe, A. Maignan, M. Hervieu, F. Damay, C. Martin, and B. Raveau, Appl. Phys. Lett. **71**, 3907 (1997).
[18] H. Sakai, K. Ito, T. Nishiyama, Xiuzhen Yu, Y. Matsui, S. Miyasaka, Y. Tokura, J. Phys. Soc. Jpn. **77**, 124712 (2008).
[19] Indu Dhiman, A. Das, A. K. Nigam, R. K. Kremer, Journal of Magnetism and Magnetic Materials, **334**, 21 (2013).
[20] Chengliang Lu, Ni Hu, Ming Yang, S. Xia, H. Wang, J. Wang, Z. Xia, and J. M. Liub, Sci. Rep., **4**, 4902 (2014).
[21] K. Pradhan, A. Mukherjee and P. Majumdar, Europhys. Lett. **84**, 37007 (2008).
[22] S. Hebert, A. Maignan, C. Martin and B. Raveau, Solid State Commun. **121** 229 (2002).
[23] E. Dagotto, T. Hotta, and A. Moreo, Phys. Rep. **344**, 1 (2001).
[24] E. Dagotto, S. Yunoki, A. L. Malvezzi, A. Moreo, J. Hu, S. Capponi, D. Poilblanc, and N. Furukawa, Phys. Rev. **B 58**,6414 (1998).
[25] K. Pradhan, A. Mukherjee and P. Majumdar, Phys. Rev. Lett. **99**, 147206 (2007).
[26] S. Kumar and P. Majumdar, Eur. Phys. J. **B 50**, 571 (2006).
[27] Sanjeev Kumar, Arno P. Kampf, and Pinaki Majumdar, Phys. Rev. Lett. **97**, 176403 (2006).
[28] Sanjeev Kumar and Arno P. Kampf, Phys. Rev. Lett. **100**, 076406 (2008).
[29] K. Pradhan, Arno P. Kampf, Phys. Rev. **B 88**, 155136 (2013).
[30] Seiji Yunoki, Takashi Hotta, and Elbio Dagotto, Phys. Rev. Lett. **84**, 3714 (2000).
[31] S. Fratini, D. Feinberg, and M. Grilli, Eur. Phys. J. **B 22**, 205110 (2001).
[32] Vijay B. Shenoy, Tribikram Gupta, H. R. Krishnamurthy, and T. V. Ramakrishnan, Phys. Rev. Lett. **98**, 097201 (2007).
[33] F. studer, O. Toulemonde, J. Goedkoop, A. Barnabe, and B. Raveau, Jpn. J. Appl. Phys. **38**, 377 (1999).
[34] The SE interaction is dependent on t scale and Hubbard repulsion U as t^2/U. In case of Fe^{3+} ($t_{2g}^3 e_g^2$), the U is large as the next electron goes to a t_{2g} level. For Cr^{3+} ($t_{2g}^3 e_g^0$) the effective U is probably smaller, which is why Cr has a stronger SE coupling to Mn than Fe does.